Article Submitted to Bulletin of Mathematical Biology

Pattern Formation in Reaction-Diffusion Models with Nonuniform Domain Growth

E. J. CRAMPIN[1], W. W. HACKBORN[2] AND P. K. MAINI[1]

[1] *Centre for Mathematical Biology, Mathematical Institute, University of Oxford, 24–29 St Giles', Oxford OX1 3LB, UK*

[2] *Augustana University College, Mathematical Sciences Division, 4901 – 46th Avenue, Camrose, Alberta, Canada, T4V 2R3*

Abstract

Recent examples of biological pattern formation where a pattern changes qualitatively as the underlying domain grows have given rise to renewed interest in the reaction-diffusion (Turing) pattern formation model. Several authors have now reported studies showing that sequences of patterns consistent with experimental observations can be generated by the Turing model with domain growth, demonstrating the tendency for temporally regular and spatially symmetrical splitting or insertion of concentration peaks in response to growth of the underlying domain. This has also been suggested as a mechanism for increased pattern selection reliability. However, thus far authors have only considered the restricted case where growth is uniform throughout the domain.

In this paper we generalise our recent results for reaction-diffusion pattern formation on growing domains to consider the effects on pattern formation of growth that is not spatially uniform. The purpose is twofold: firstly to demonstrate that the addition of *weak* spatial heterogeneities does not change the conclusions reached for pattern formation on growing domains, but secondly that sufficiently *strong* nonuniformity, for example where only one part of a larger domain is expanding, can give rise to sequences of patterns not seen for the uniform case, and gives a further mechanism for controlling pattern selection. A framework for modelling is presented in which domain expansion and boundary (apical) growth are unified in a consistent manner. The results have implications for all reaction-diffusion type models subject to underlying domain growth.

1. Introduction

Pattern formation in reaction-diffusion systems is the paradigm for models of spatial self-organisation, and following its proposal by Turing in 1952, the theory

has found many applications in modelling biological pattern formation. Traditionally models consider the formation of pattern under the pre-pattern assumption, that spatial pattern is initially established in the concentration of some chemical (or morphogen) and only subsequently, and on a longer timescale, are these patterns interpreted for cellular differentiation (as positional information). Recently several examples of biological pattern formation have been described where an observed pattern changes qualitatively as the underlying domain grows, suggesting that the pattern formation process in these examples is commensurate with growth of the domain which is being patterned.

Turing (1952) proposed that pattern formation during morphogenesis might arise through an instability in systems of reacting chemicals, driven by diffusion. A set of two or more chemicals is required to interact in a well defined manner in order that heterogeneous patterns may arise in their concentrations. Significantly, for the spatially homogeneous state to be stable in the absence of diffusion yet unstable to spatial perturbations of particular wavelengths (diffusion-driven instability, DDI) disparity is required between the diffusivities of the chemicals. The pattern forming interaction between two such chemicals has been described in terms of short range auto-catalytic activation and long range (lateral) inhibition by Gierer and Meinhardt (1972), and in two-species models the chemical components are referred to as the activator and the inhibitor species. Linear stability analysis (Murray, 1993) of the homogeneous steady state shows that the inhibitory chemical must have larger diffusivity than the self-activating one.

Renewed impetus was recently provided by Kondo and Asai (1995), who suggested that a reaction-diffusion mechanism could be responsible for the dynamic changes in pigmentation patterns of the marine angelfish *Pomacanthus*. Unlike mammalian coat markings, the pattern in the skin of these fish changes dynamically during growth of the animal, rather than simply enlarging in proportion to the body size. Juvenile *P. imperator* display concentric stripes and *P. semicirculatus* have a regular array of vertical stripes which increase in number during growth. Juvenile *P. semicirculatus* of less than 2cm in length display three vertical stripes which separate until the length of the fish is approximately 4cm, at which point new stripes appear between the original ones. Similarly at around 8-9cm in length new stripes again appear between the existing ones. In this manner the pattern changes by insertion of new stripes as the animal roughly doubles in length, to preserve the wavelength of the pattern. In *P. imperator* this behaviour is maintained in the adult fish, where horizontal stripes maintain an average spacing. This dynamic regulation of pattern is quite unlike the static pattern selection problem classically studied for the reaction-diffusion system.

The numerical computations of Kondo and Asai (1995), subsequently confirmed and extended by Painter et al. (1999), show that this sequence of patterns is reproduced by reaction-diffusion schemes on growing domains, with the pattern wavelength conserved when the domain length is doubled, called frequency-doubling (FD, equivalent to mode-doubling on the dimensional domain). Transitions between patterns arise through one of two mechanisms, insertion (as for

the fish) or splitting of activator peaks, and in special circumstances these mechanisms operate together (frequency-tripling, see Crampin et al., 2001). Patterns evolving on the growing domain follow a sequence which depends on the initial pattern to form, but is otherwise insensitive to initial conditions, and hence it has been suggested that this is a mechanism for reliable pattern generation (Crampin et al., 1999).

Domain expansion has previously been considered in reaction-diffusion models for the branching morphology of growing *Micrasterias* (Lacalli, 1981) and for the emergence of tooth primordia in the alligator (Kulesa et al., 1996). Here experimental evidence suggests that the spatial positioning and order of appearance of tooth primordia is determined in part by tissue growth throughout the jaw. Recently it has been suggested that reaction-diffusion pre-patterns may be important in the growth and development of solid tumours (Chaplain et al., 2001), and in ligament patterning in certain bivalves (Madzvamuse et al., 2001).

Biologically there may be many underlying reasons for nonuniformity in domain growth. For example, signalling cues which determine the local growth rates (such as growth factors, or other chemicals) may not be uniformly distributed throughout the tissue. In such cases the local strain rate will depend on position (as well as time). Also, it is biologically plausible that the reacting and diffusing chemicals may themselves be responsible for the local determination of the growth, so that the local expansion rate is a function of their concentrations, a situation we call reactant-controlled growth. One further scenario which can be studied is that of apical growth, for example in developing shells (Meinhardt, 1995) and at the apical meristem in plants, where patterning occurs behind an outgrowing region at the boundary of the domain.

In this paper we investigate the formation of pattern sequences in the Turing reaction-diffusion model under such nonuniform conditions. In particular we would like to know whether introducing weak nonuniformity (where there is slow quantitative change in the growth across the domain) disrupts the regular frequency-doubling sequence, or whether the sequence is robust to such changes. Furthermore, we are interested in whether suitably chosen and sufficiently strong nonuniformity (such that one section of the domain is growing in a quite different manner or rate to another part) can produce reliable sequences other than frequency-doubling. In the following section we present the modelling framework, which is then used in the subsequent sections to illustrate pattern selection under uniform, apical and finally nonuniform growth conditions.

2. Model Derivation

The evolution equations for the reaction-diffusion processes on a growing domain are readily obtained from consideration of mass conservation. Rather than considering one particular case, we present a general framework which will allow subsequent inclusion of the detailed properties of any specific tissue. Conse-

quently the derivation of the governing equation is considered as a problem in kinematics, and no constitutive equations are proposed.

Specifically, we assume that the domain undergoes deformation and expansion with no accompanying change in density (incompressibility condition). Growth consists of local directional volume expansion resulting in the transport of material. In what follows we will consider only planar domains, however, it is clear that domain curvature, both stationary and changing in time, are potentially important influences on pattern formation, in particular in the biological context.

Reaction diffusion systems of the type studied for pattern formation generally exclude cross-diffusion, and are coupled only in the kinetic terms. Hence we may consider the kinematics for a single substance with straightforward generalisation to a system of interacting chemicals. Growth of the domain $\mathbf{x} \in \Omega(t)$ with boundary $\partial\Omega(t)$ generates a flow $\mathbf{a}(\mathbf{x}, t)$. Application of the Reynolds Transport Theorem to the equation of mass conservation for a substance C which diffuses with constant-density diffusivity D_c and undergoes reaction at rate R gives

$$\frac{\partial c}{\partial t} + \nabla \cdot (\mathbf{a}\, c) = D_c \nabla^2 c + R(c, \mathbf{x}, t) \tag{1}$$

where $c(\mathbf{x}, t)$ is the concentration at position $\mathbf{x}$ and time t. The coupling to other substances, which may also diffuse, is through the reaction term $R(c, \mathbf{x}, t)$. The time varying domain introduces two new terms to the standard reaction-diffusion equation: transport of material around the domain at a rate determined by the flow, $\mathbf{a} \cdot \nabla c$, and the diluting (concentrating) effect of local volume increase (decrease), $c \nabla \cdot \mathbf{a}$.

2.1. Nondimensionalisation

The Turing instability requires the interaction of (at least) two substances, (u, v), giving a system of equations of the above form coupled through the kinetic terms $f(u, v)$ and $g(u, v)$. Before nondimensionalising, the system is standardised by ordering the variables in terms of decreasing diffusivity such that $D_u \geq D_v$, and the activating species is labelled as v. Introducing nondimensional variables for concentration, position and time leads to the nondimensional system

$$\frac{\partial u}{\partial t} + \nabla \cdot (\mathbf{a}\, u) = \frac{1}{\gamma_0} \nabla^2 u + f(u, v) \tag{2}$$

$$\frac{\partial v}{\partial t} + \nabla \cdot (\mathbf{a}\, v) = \frac{d}{\gamma_0} \nabla^2 v + g(u, v) \tag{3}$$

where $d = D_v / D_u \leq 1$ is the ratio of diffusivities, $\gamma_0 = \omega L^2 / D_u$ is a dimensionless parameter which represents the ratio of diffusive T_D to kinetic T_R relaxation times, $T_D = L^2 / D_u$ and $T_R = 1/\omega$, L is a length scale (the initial domain length in the one-dimensional case) and ω is a reaction rate. Typically, no-flux conditions are imposed on the domain boundary

$$\nabla u = \nabla v = 0 \quad \text{on} \quad \mathbf{x} \in \partial\Omega(t). \tag{4}$$

2.2. Determining the Flow

The flow $\mathbf{a}$ may be specified directly for certain simple cases. However, in general $\mathbf{a}(\mathbf{x}, t)$ will be determined by an extended system of constitutive equations describing the properties of the tissue. We will assume that growth properties are determined locally due to factors that will not be explicitly modelled, but which might include the effects of growth factors and cellular or sub-cellular structures giving rise to mechanical anisotropy, influencing the direction of growth. Such properties will be specified on an initial position $\mathbf{X}$ and subsequently follow the flow due to tissue growth. Lagrangian coordinates, $(\mathbf{X}, t)$, are therefore a very natural system in which to work. Tissue movement is described in terms of the trajectories $\mathbf{\Gamma}$ of elemental tissue volumes

$$\mathbf{x} = \mathbf{\Gamma}(\mathbf{X}, t) = \big(\Gamma_1(\mathbf{X}, t), \Gamma_2(\mathbf{X}, t), \Gamma_3(\mathbf{X}, t)\big). \tag{5}$$

Solid body translations and rotations of the domain leave the pattern generated by reaction and diffusion within the tissue unaffected. The coordinates for the domain are chosen such that there is a reference point which is initially at the origin of the coordinate system and which remains at the origin during the subsequent flow. Some general conditions must then be observed for the components of $\mathbf{\Gamma}$. From the definition of $\mathbf{\Gamma}$, the initial condition is

$$\mathbf{\Gamma}(\mathbf{X}, 0) = \mathbf{X}. \tag{6}$$

In the absence of solid body translations we also have the boundary condition $\mathbf{\Gamma}(\mathbf{X}_r, t) = \mathbf{X}_r$ for reference point $\mathbf{X}_r$, and choosing the coordinate system such that the point of reference is the origin, $\mathbf{X}_r = \mathbf{0}$, leads us to require

$$\mathbf{\Gamma}(\mathbf{0}, t) = \mathbf{0}. \tag{7}$$

The deformation of the tissue due to growth in N-dimensions is described by the $N \times N$ rate of deformation tensor L_{ij} where the components are determined by local tissue properties. The antisymmetric part of this tensor is associated with rigid body rotation and so we assume that L_{ij} is symmetric, describing the tissue strain rate. Off diagonal elements of L_{ij} correspond to the shear rate between axes x_i and x_j with no accompanying volume change. On-diagonal components give the rate of extension along each axis and the trace

$$\sum_{i=j} L_{ij} = \nabla \cdot \mathbf{a} = S(\mathbf{X}, t) \tag{8}$$

gives the rate of volume expansion, thus for domain *growth* we must have $S(\mathbf{X}, t) > 0$ (and hence $c\nabla \cdot \mathbf{a}$ is a *dilution* term). $L_{ij}(\mathbf{X}, t)$ is related to coordinates $(\mathbf{X}, t)$ via

$$\frac{\partial^2 \Gamma_i}{\partial t \, \partial X_k} = \sum_j L_{ij} \frac{\partial \Gamma_j}{\partial X_k} \tag{9}$$

from which in general we can calculate $\mathbf{\Gamma}(\mathbf{X}, t)$ and thus the flow, $\mathbf{a}$, due to the domain growth.

In the following sections we consider several specific cases, where we assume the form of the components of L_{ij} and from them derive the trajectories, $\mathbf{\Gamma}$, and the flow, $\mathbf{a}$. Firstly we consider the general form taken for the evolution equation for one spatial dimension.

2.3. One-dimensional Growth

In this paper we will present results in one spatial dimension. Specification of the local growth characteristics reduces to specifying the sole component of the tensor, strain rate $L_{11} = S(X, t)$. The trajectories, found by integrating equation (9) with $i, j, k = 1$ using conditions (6) and (7), are

$$\Gamma(X, t) = \int_0^X \left[\exp \int_0^t S(z, \tau)\, \mathrm{d}\tau \right] \mathrm{d}z \tag{10}$$

and the flow $a(X, t) = \partial\Gamma/\partial t$. To isolate the effects of transport within the domain and to facilitate comparison of results, we transform the spatial coordinate to the unit interval using the uniform spatial scaling $\xi = x/r(t) \in [0, 1]$, where

$$r(t) = \Gamma(1, t) \tag{11}$$

is the nondimensional domain length, and the transformed evolution equation is

$$u_t = \frac{1}{\gamma(t)} u_{\xi\xi} + \chi(\xi, t)\, u_\xi + f(u, v) - S(\xi, t)\, u \tag{12}$$

$$v_t = \frac{d}{\gamma(t)} v_{\xi\xi} + \chi(\xi, t)\, v_\xi + g(u, v) - S(\xi, t)\, v \tag{13}$$

with $\gamma(t) = \gamma_0 \big(r(t)\big)^2$ and

$$\chi(\xi, t) = \frac{1}{r(t)} \big(\xi \dot{r}(t) - a(\xi, t) \big) \tag{14}$$

where $\dot{r}$ represents the time derivative of r.

2.4. Timescales: Slow Domain Growth

Domain growth introduces a new timescale to the problem through the rate of volume expansion. We denote this explicitly writing

$$\| S(\mathbf{X}, t) \| \sim \rho. \tag{15}$$

The effect of growth on pattern formation is expected to depend on the relative magnitudes of the timescales for domain growth and pattern formation. Having nondimensionalised time using the kinetic relaxation time T_R, spatial pattern is

established on a timescale of $\mathcal{O}(1)$, and hence $1/\rho$ measures the time for domain growth relative to pattern formation. For biological systems we suggest that reaction and diffusion processes will operate on a much faster timescale than the cellular machinery involved in tissue growth, and thus the relevant regime is one in which

$$0 < \rho \ll 1. \tag{16}$$

In this case the dilution term is small compared to any $\mathcal{O}(1)$ linear terms in the reaction kinetic functions.

2.5. Reaction Schemes

Two different reaction schemes which illustrate the two mechanisms for pattern transition: splitting (Schnakenberg kinetics) and insertion (Gierer-Meinhardt kinetics) of activator peaks, are presented briefly below. These mechanisms for pattern transitions have been investigated in a class of reaction-diffusion systems by Crampin et al. (2001), wherein a third mechanism is also described for which splitting and insertion occur simultaneously.

Schnakenberg (1979) proposed a hypothetical series of trimolecular autocatalytic reactions, for which the nondimensionalised concentrations of self-activating, v, and self-inhibiting, u, species give the kinetic scheme

$$f(u,v) = b - uv^2, \qquad g(u,v) = a + uv^2 - v. \tag{17}$$

Gierer and Meinhardt (1972) presented a model for pattern formation to explain the regenerative properties of hydra observed in various transplantation experiments. The kinetics are based on biologically plausible arguments and functions were chosen to reproduce the experimentally observed behaviour. The scheme considers autocatalytic activation of chemical v and self-inhibition of u and can be written as

$$f(u,v) = v^2 - u, \qquad g(u,v) = \frac{v^2}{u} - kv + \delta. \tag{18}$$

We note that equation (17) is actually a special case of one of the several different reaction schemes presented in the paper by Gierer and Meinhardt (1972).

3. Uniform Domain Growth

Before considering the effects of a strain rate that varies with position we review results for the simple case when the strain rate $S(t)$ is uniform across the domain. The trajectories are

$$\Gamma(X,t) = X \exp \int_0^t S(\tau)\,\mathrm{d}\tau = Xr(t) \tag{19}$$

and so in this case $\xi = X$ and, with $a = X\dot{r}$, the convection terms in equations (12–13) vanish under the uniform spatial scaling, $\chi = 0$, as would be expected for uniform growth. Below we present solutions for constant strain rate $S = \rho$ (see Crampin et al., 1999, for results with time-dependent strain rate). In this case the evolution equations are classical reaction-diffusion modified by a constant dilution term and time-dependent diffusivity. The two generic solution behaviours, spatial frequency-doubling via splitting and insertion of new peaks in the activator solution, are illustrated in figure 1. Note that the insertion of peaks here is consistent with the description of Kondo and Asai (1995) for the growing angelfish.

[Figure 1 about here.]

In the case of general nonuniform domain growth, $\Gamma(X,t)$ is a non-separable function of X and t: the convection term is not removed under a uniform transformation and may therefore influence pattern formation in the system. In order to investigate pattern formation under non-uniform domain growth we must consider specific examples. In section 5 we consider the one-dimensional problem comprising two sub-domains each with uniform but different growth rates, the *piecewise uniform* case, to gain some insight into the complexities of pattern sequence generation under more general growth functions. First we look at the case where growth is restricted to a region at the extending tip of the domain.

4. Apical Growth

In many developmental systems tissue growth is restricted to a region located towards a tip or boundary (at least, growth in this region is much faster than elsewhere). Pattern formation takes place behind this advancing boundary. Examples of such apical growth include the vertebrate limb bud, where rapid cell proliferation is maintained in the progress zone, a region of undifferentiated mesenchyme beneath a bounding ridge (the apical ectodermal ridge) at the tip of the limb bud. The progress zone is thought to be maintained by signals produced in specialized regions of the tissue (from the apical ectodermal ridge and the zone of polarizing activity, a region at the posterior margin of the limb bud), and the rapid proliferation remains localised close to the border of the limb bud during outgrowth. Similarly, in plants, growth typically occurs at the apex of an outgrowing shoot (at the shoot apical meristem), from which organs such as leaves and flower buds originate.

For a proliferating region that retains a constant cell population the rate of outgrowth will be determined by the proliferation rate and the cell population size of that region. We model this by assuming strain rate $S_{tip}(t)$ in the proliferating region maintained at width δ, and zero growth elsewhere, hence

$$S(x,t) = \begin{cases} 0, & 0 \le x < r(t) - \delta \\ S_{tip}(t), & r(t) - \delta \le x \le r(t) \end{cases} \tag{20}$$

Integrating, and transforming uniformly we find that the flow

$$a(\xi,t) = \begin{cases} 0, & 0 \le \xi < 1 - \delta/r(t) \\ \big((\xi-1)\,r(t) + \delta\big) S_{tip}(t), & 1 - \delta/r(t) \le \xi \le 1 \end{cases} \tag{21}$$

where $r(t) = 1 + \delta \int_0^t S_{tip}(\tau)\mathrm{d}\tau$ is the dimensionless domain length.

In the limit that the proliferating region is much smaller than the remainder of the domain, the system can be reduced to a moving boundary problem. Formally this can be shown by choosing $\|S\| \sim 1/\delta$ as $\delta \to 0$. Then the flow is zero everywhere (the proliferating region is vanishingly small), however, the domain length $r(t) \sim \mathcal{O}(1)$ and increases with time. In this limit the scaled reaction-diffusion system becomes

$$u_t = \frac{1}{\gamma(t)} u_{\xi\xi} + \xi \frac{\dot{r}(t)}{r(t)} u_\xi + f(u,v) \tag{22}$$

$$v_t = \frac{d}{\gamma(t)} v_{\xi\xi} + \xi \frac{\dot{r}(t)}{r(t)} v_\xi + g(u,v) \tag{23}$$

Solution behaviour for constant proliferation rate, $S_{tip} = \rho \ll 1$, is shown for both splitting and insertion in figure 2.

[Figure 2 about here.]

Meinhardt et al. (1998) considered a similar model in two spatial dimensions for the generation of the arrangements of leaves found on plant stems (phyllotaxis). In computer simulations the growing plant stem is idealised as a cylindrical domain with the addition of cells parallel to the axis of the cylinder. Various of the commonly observed morphologies for leaf primordia may be generated by varying the diffusion constants and the growth rate ρ. A similar model has also been developed for the pigmentation patterns of some sea shells, which also grow from a narrow region near the leading edge of the shell (Meinhardt, 1995). Here we have shown how such moving boundary models can be incorporated into the general framework, as a special case of nonuniform domain growth.

5. Nonuniform Domain Growth

To investigate in greater depth the role of nonuniformity in the domain growth we firstly consider a simplified scenario in which a one-dimensional domain comprises two sub-domains, each undergoing slow uniform domain growth but with different strain rates. This problem is studied in detail with the aim of gaining insight into the possibilities and complexities of pattern sequences generated under more general nonuniform growth conditions.

We define $S(X,t)$ on the two sub-domains

$$S(X,t) = \begin{cases} S_1(t), & 0 \le X \le \Theta \\ S_2(t), & \Theta < X \le 1 \end{cases} \tag{24}$$

where Θ is the dimensionless initial position of the interface between the two sub-domains. Trajectories are calculated from equation (10)

$$\Gamma(X,t) = \begin{cases} Xr_1(t), & 0 \le X \le \Theta \\ \Theta\big(r_1(t) - r_2(t)\big) + Xr_2(t), & \Theta < X \le 1 \end{cases} \tag{25}$$

where $r_i(t) = \exp \int_0^t S_i(\tau)\mathrm{d}\tau$, from which we can calculate the flow directly. The latter, when scaled, is given by

$$a(\xi,t) = \begin{cases} \xi\dfrac{\dot{r}_1}{r_1}r(t), & 0 \le \xi \le \theta(t)/r(t) \\ \theta(t)\left(\dfrac{\dot{r}_1}{r_1} - \dfrac{\dot{r}_2}{r_2}\right) + \xi\dfrac{\dot{r}_2}{r_2}r(t), & \theta(t)/r(t) < \xi \le 1 \end{cases} \tag{26}$$

Due to the growth of the left-hand sub-domain ($i = 1$) there is a moving interface between the sub-domains $\theta(t) = \Theta r_1(t)$ and the total domain length is given by

$$r(t) = \Theta r_1(t) + (1 - \Theta)\, r_2(t). \tag{27}$$

The advective terms in the equations arise despite the uniformity of growth for each sub-domain because of the choice of spatial transformation, also giving rise to the internal moving boundary.

Below we present results for constant strain rate in each sub-domain, $S_i = \rho_i \ll 1$ for $i = 1, 2$. Then $a \sim \mathcal{O}(\rho)$ and $\dot{r}(t) \sim \mathcal{O}(\rho)$, and given that $r(t) \ge 1$ while $\xi \in [0, 1]$ we also find that $\chi \sim \mathcal{O}(\rho)$ or smaller, so that the advection component is small. Numerical solutions were computed by discretising the domain to deal with the internal boundary and then integrating the resulting system of coupled ordinary differential equations forward in time, as described in the Appendix. Continuity of flux at the interface permits communication between the two regions. Pattern formation on each sub-domain will influence the solution behaviour on the other and so we expect that the pattern sequence may differ from the case of uniform growth across the whole domain. In the figures the location of the interface between the uniformly growing sub-domains is shown by the dashed line.

[Figure 3 about here.]

Comparison with the pattern formed under uniform growth, figure 1(b), shows that piecewise uniform growth at relatively high strain rate generates asymmetry in peak splitting (figure 3). This is similar to the asymmetries observed for high strain rates for uniform domain growth reported in Crampin et al. (1999). This represents a smooth modulation of the frequency-doubling sequence. Each peak still undergoes splitting. For lower strain rates peaks occasionally fail to split, even when the strain rates for the two sub-domains are very close (figure 4).

[Figure 4 about here.]

This defect in the peak splitting is reminiscent of the breakdown of the frequency doubling sequence at very low uniform strain rates (Crampin et al., 1999), however, introduction of a continuous strain rate function $S(X,t)$ (below) suggests that this is an effect of the discontinuity in the piecewise constant strain rate.

When only one sub-domain is growing, similar to apical growth, there is a strong tendency for peak splitting to be restricted to the growing region (figure 5(a)).

[Figure 5 about here.]

Here any tissue originating from the growing sub-domain continues to expand, in contrast to the apical problem in which growth is restricted to a region of predetermined size. If the initial domain size is increased so that activator peaks form simultaneously on the growing and non-growing sub-domains (figure 5(b)), different sequences can be generated. In this example, two peaks transform to three via splitting on the growing sub-domain, and subsequently six peaks are formed when the peak closest to the interface splits. However, the tendency for peaks only to split on the growing part is sustained. At lower strain rate this differentiation between growing and non-growing regions appears even more distinct (figure 6). Figure 6(a) has model parameters identical to figure 5(b) but with reduced strain rate.

[Figure 6 about here.]

These results are corroborated by solving the equations for nonuniform domain growth taking the *tanh* function to approximate the discontinuous step in strain rate

$$S(X,t) = \rho_1 + \frac{(\rho_2 - \rho_1)}{2}\left[1 + \tanh\left(\frac{X-\Theta}{\varepsilon}\right)\right] \tag{28}$$

which tends to a step-function between ρ_1 and ρ_2 centred on $X = \Theta$, as $\varepsilon \to 0$. Numerical solutions for this strain rate function are computed by writing the evolution equations in Lagrangian form (see Appendix). For high values of the strain rate, i.e $\rho_i \sim 0.01$, there is little difference between the solutions for strain rate given by equation (28) and for piecewise uniform strain rate, even when the change is very gradual ($\varepsilon \sim 1$). As the strain rate is decreased, the piecewise uniform growth results are recovered as $\varepsilon \to 0$. Figure 7 shows activator solutions with ρ_1 and ρ_2 the same as in figure 4(a) for decreasing ε.

[Figure 7 about here.]

Whereas regular peak splitting is seen for larger ε, certain peaks fail to split as ε decreases and $S(X,t)$ becomes increasingly step-like.

Results of simulations with larger initial domain size are presented in figure 8.

[Figure 8 about here.]

Here $\rho_1 = 0$ and as $\varepsilon \to 0$ the left hand part of the domain is not growing. The same behaviour as for the piecewise uniform case is seen in the limit (only when $\varepsilon \approx 0$ is S close to zero in the left hand side of the domain), and for each solution the transition from two to three peaks is observed as only the peak in the region of faster domain growth splits. These results indicate that the transition from two activator peaks to three on the growing domain is not strongly dependent on the exact nonuniformity.

6. Reactant-Controlled Growth

Several models have been proposed in the literature for which domain growth is determined by reaction-diffusion variables. Dillon and Othmer (1999) study pattern formation in the growing limb bud, modelled as an incompressible fluid with a distributed source term which is a function of the local chemical composition. In their model there are two chemical components which react and diffuse through the growing fluid region, however, their system is not of Turing-type and only simple gradients in the chemicals are formed. Modelling the morphogenesis of green algae, Harrison and Kolář (1988) and Holloway and Harrison (1999) couple a Turing mechanism to domain growth. Their study is extended to two- and three-dimensional domains (Harrison et al., 2001). However, they also include a feedback mechanism to the kinetics such that the diffusion-driven instability operates only within history-dependent boundaries separated by 'inert' regions for which there is no pattern formation.

The coupling of domain growth to the chemical kinetics provides a feedback between the pattern formation process and the mechanism that generates sequences of patterns. As an example, we consider a model for which domain growth is controlled by 'growth factor' v, the self-activating component. Rather than model a specific biochemical pathway, we will assume functional forms for the uptake of the growth factor, $\Delta(v)$, and the response function which determines the local growth, $S(v)$. If uptake of v is limited by receptor saturation then we expect the relationship to be sigmoidal. A similar problem arises in the biological chemostat (continuously-stirred tank reactor, CSTR, see for example Smith and Waltman (1995)) in which nutrient is supplied to a well-mixed tank containing a micro-organism population (with possibly several interacting species). The empirical relationship observed between population growth and nutrient consumption is sigmoidal (Monod, 1942). Therefore in the absence of other detailed information, we take

$$\Delta(v) = \frac{\alpha v}{\kappa + v}, \qquad S(v) = \frac{\rho v}{\kappa + v} \tag{29}$$

where the growth response is on a slow timescale, $\rho \ll 1$. The assumption that tissue density remains constant (incompressibility) implies that the result of tissue growth, increased cell size or proliferation, is expansion of the domain,

and the evolution equation is

$$u_t = \frac{1}{\gamma(t)} u_{\xi\xi} + \chi(\xi, t)\, u_\xi + f(u, v) - \frac{\rho u v}{\kappa + v} \tag{30}$$

$$v_t = \frac{d}{\gamma(t)} v_{\xi\xi} + \chi(\xi, t)\, v_\xi + g(u, v) - \frac{(\rho v + \alpha) v}{\kappa + v} \tag{31}$$

where γ and χ are defined as above (equation (14)). Numerical solutions presented in figure 9 were computed by casting the equations in Lagrangian form (see Appendix), for which explicit calculation of the kinematic flow in the domain is not required. The strain rate S is plotted as a function of time and scaled space in figure 9(b), where those parts of the domain which are growing are shaded dark, and is seen to correspond closely to the evolving activator profile.

[Figure 9 about here.]

The regular doubling of the number of peaks on the domain is unsurprising in light of the results described above as S has no discontinuities and is significantly greater than zero in positions that coincide with the location of the peaks. The trajectories of particles embedded in the domain (flow lines), uniformly scaled to the unit interval, $\Gamma(X, t)/\Gamma(1, t)$ for different values of the initial position X, are plotted in figure 10 in which the relative expansion of different regions of the domain can be seen.

[Figure 10 about here.]

7. Discussion

For those cases above for which only Schnakenberg results are shown, analogous results obtain for insertion in Gierer Meinhardt kinetics. There is no significant effect on pattern amplitude or wavelength from the spatial dependence of terms in the equation for nonuniform growth. For slow domain growth the advective term is correspondingly small, and peaks in the activator concentration reorganise continuously to maintain separation which is roughly independent of position. In figures 3 and 5 the asymmetry in the pattern is due to the relatively high value of ρ. Here peaks do not reach their stationary positions during separation subsequent to splitting, before the domain is sufficiently large for the peaks to undergo the next transition. For slower domain growth (figures 4 and 6) the nonuniformity of the domain growth is reflected in the failure of some peaks to split, giving an asymmetric sequence of patterns.

Nonuniformity in the domain growth introduces terms with explicit spatial dependence into the evolution equation. In its original formulation, and in most subsequent development, the theory of pattern formation in reaction-diffusion equations assumes homogeneity in parameters throughout the domain, for the good reason that DDI generates inhomogeneity where before there was none.

Indeed, this is the source of much of the theoretical interest in such pattern forming instabilities. One exception is the analytical study of a reaction term with explicit space-dependence by Auchmuty and Nicolis (1975) (see also the numerical simulations of Herschkowitz-Kaufman, 1975). Also, the recent interest in the modelling of chemical pattern formation in gel reactors leads to the study of spatial gradients in certain reaction terms. In the Gel Strip reactor the feed of the reactants, held at fixed concentrations at the boundaries, establishes steady gradients across the domain of pattern formation. Theoretical studies prior to the experimental realisation of Turing patterns in gel reactors are given by Dewel and Borckmans (1989) and modelling of the structures experimentally observed in these ramped systems is presented by Borckmans et al. (1992) and Dulos et al. (1996).

In several applications of the theory to problems in biological pattern formation, authors have considered some underlying spatial dependence. For example, Gierer and Meinhardt (1972) include a shallow source gradient in their model for morphogenesis and regeneration in Hydra to orient patterns (by removing degeneracy in the spatial modes). Benson and co-authors have demonstrated that inhomogeneous reaction-diffusion equations may generate patterns with continuously varying amplitude (Maini et al., 1992) (see also May et al., 1999) and wavelength (Benson et al., 1993) when one or both diffusion parameters are varying in space. In our equations for nonuniform domain growth the spatially-dependent terms are small, due to the small parameter arising from the different timescales, and so we do not expect strong influence on the amplitude or wavelength of patterns generated by the model.

We now reassess the two questions that were posed at the beginning. We have shown that for small spatial perturbation, which we interpret as gentle gradients in the spatial dependence, we recover FD-type sequences (at least for the low modes that we have monitored). For more *strongly* nonuniform growth (for steeper change in S) at high ρ we have observed asymmetry, as for the uniform case, and for lower ρ selected peaks fail to undergo transitions, akin to the failure of FD for uniform linear growth. For highly nonuniform domain growth, and in particular when one region of the domain is not growing, other sequences may be formed by the failure of peak splitting (or insertion) at particular locations, specifically for those peaks on the stationary part. This mechanism also appears to some degree robust, suggesting that it may be possible to choose the nonuniformity such that a specific pattern is selected during domain growth (as part of an evolving sequence) and furthermore, that the same pattern will be selected for some amount of variation of the nonuniformity.

Clearly for a thorough investigation of the potential for pattern selection on growing domains and its relation to biological settings, results in two spatial dimensions, and on curved surfaces are required. Varea et al. (1999) have considered pattern formation on spherical surfaces while Chaplain et al. (2001) investigate patterns on the radially growing sphere. Liaw et al. (2001) show that the patterns exhibited by a Turing reaction-diffusion system on a fixed portion

of a sphere resemble closely those observed on lady beetles (ladybirds). Moreover, their preliminary study suggests that curvature does not alter significantly the results for the case of planar domains. Clearly the formalism that we have described can be adapted to encompass these and other geometries. Indeed, this has been done in parallel to the work presented here (Plaza et al., 2001).

It also remains to be seen as to whether the behaviour we have described is particular to reaction-diffusion systems or is generic to all global pattern generation mechanisms (where the pattern forming dynamical system acts globally across the whole domain), such as chemotaxis and cell motility (mechano-chemical) models. From a mathematical viewpoint it has been shown that models which differ widely in their physical interpretation may nevertheless exhibit very similar behaviour, suggesting that predictions can be made that are mechanism-independent (Oster and Murray, 1989). In terms of the phenomenology of patterns generated on fixed domains, such mechanisms are difficult to distinguish, all having a range of destabilising modes which present the same pattern selection issues and similar robustness problems, leading to model predictions that are independent of the detailed underlying biology. If such models are found to differ under domain growth then the predicted behaviour on the growing domain will provide a useful means to distinguish between them experimentally, when trying to identify which biological pattern formation events might arise as a consequence of a reaction-diffusion mechanism, and where it may be more prudent to seek alternative explanation. Whether these other models exhibit qualitatively different behaviour in response to domain growth is the subject of current investigation.

Appendix

Numerical Solution for Piecewise Uniform Growth

Reactant concentrations $u(\xi,t)$ and $v(\xi,t)$ and their fluxes are continuous at the moving internal boundary $\xi = \theta(t)/r(t)$ between the two sub-domains. The effective diffusion coefficients are functions of time through $\gamma(t)$ but are independent of ξ, thus continuity of flux requires that the first spatial derivatives are continuous across the internal boundary. The spatial interval is discretised with a uniform mesh, writing $U_i(t) \approx u(\xi_i,t)$ as the approximate values of the solution $u(\xi,t)$ at the mesh points ξ_i, $i = 1,2,\ldots,N$, and similarly $V_i(t) \approx v(\xi_i,t)$. The first spatial derivative is approximated using standard central differences. Central differences are also taken for the second spatial derivative within the two sub-domains, however, the formula will not be valid across the internal boundary. We adopt the strategy often used to deal with curved boundaries (see for example Morton and Mayers, 1994) and introduce an extra mesh point, $\xi_\theta = \theta(t)/r(t)$ at the internal boundary. When $\xi_i < \xi_\theta < \xi_{i+1}$ we linearly interpolate to find an approximation, U_θ, to the solution at position ξ_θ

$$U_\theta \approx (1-\lambda_+)\,U_i + \lambda_+ U_{i+1} \tag{32}$$

where $\lambda_+ = (\xi_\theta - \xi_i)/h$ for mesh spacing h. The central differences formula for the second derivative is modified by foreshortening the range in the direction of the internal boundary

$$\left[\frac{\partial^2 u}{\partial \xi^2}\right]_{\xi_i} \approx \frac{2}{(1+\lambda_+)\,h^2}\left[U_{i+1} - 2U_i + U_{i-1}\right]. \tag{33}$$

Similar expressions are derived for $\xi_{i-1} < \xi_\theta < \xi_i$, with $\lambda_- = (\xi_i - \xi_\theta)/h$. With these formulae the system of ordinary differential equations in U_i and V_i is integrated forwards in time using Gear's method.

Lagrangian Formulation for Nonuniform and Reactant Controlled Growth

If, for strain rate S, an explicit inversion of $\Gamma(X,t)$ is not readily found then it is easier to compute numerical solutions to the Lagrangian problem. Explicit calculation of the kinematic velocity is then not required during the computation. Writing variables as functions of initial position X and time t the evolution equation becomes

$$c_t = D_c \frac{1}{\Gamma_X}\left[\frac{1}{\Gamma_X} c_X\right]_X + R(c) - S(X,t)\,c \tag{34}$$

with initial and boundary conditions for $c(X,t)$ and $\Gamma(X,t)$

$$c(X,0) = c_0(X), \qquad c_X(0,t) = c_X(1,t) = 0 \tag{35}$$

$$\Gamma(X,0) = X, \qquad \Gamma(0,t) = 0. \tag{36}$$

The transformation to Lagrangian coordinates can naturally also be made in higher spatial dimensions. These equations can be written as a system of first order partial differential equations in the variables $(u, u_X, v, v_X, \Gamma, \Gamma_X)$. Numerical solutions are found by discretising the first order system using the Keller box scheme (Morton and Mayers, 1994), implemented in the NAG library routine `D03PEF`. Solutions at equally spaced ξ or x are calculated by interpolating from the solutions at equally spaced X, for example using routine `C05AZF` to invert Γ and `E01BFF` to interpolate.

To recover the form of the pattern on the uniformly scaled domain (ξ, t) the solution is translated with the scaled trajectories $\Gamma(X,t)/\Gamma(1,t)$. The computation proceeds on a grid which is equally spaced in X, while patterns are approximately equally spaced in ξ. During growth of the domain, any particular interval in X may expand to become a large interval in ξ. Hence in order to achieve reliable results a large number of grid points is required. This is the trade-off against the computational effort saved in not inverting Γ at each step of the calculation. For the simulations presented above, we repeated the computations doubling the number of grid points to ensure that the simulation had converged.

Acknowledgements

EJC was supported by a BBSRC studentship. Part of this work was completed while EJC and PKM visited the Isaac Newton Institute for Mathematical Sciences, University of Cambridge, where PKM was a Senior Visiting Fellow.

References

J. F. G. Auchmuty and G. Nicolis. Bifurcation analysis of nonlinear reaction-diffusion equations—I. Evolution equations and the steady state solutions. *Bull. Math. Biol*, 37:323–365, 1975.

D. L. Benson, P. K. Maini, and J. A. Sherratt. Analysis of pattern formation in reaction diffusion models with spatially inhomogeneous diffusion coefficients. *Mathl. Comput. Modelling*, 17(12):29–34, 1993.

P. Borckmans, A. De Wit, and G. Dewel. Competition in ramped Turing structures. *Physica A*, 188:137–157, 1992.

M. A. J. Chaplain, M. Ganesh, and I. G. Graham. Spatio-temporal pattern formation on spherical surfaces: Numerical simulation and application to solid tumour growth. *J. Math. Biol*, 42(5):387–423, 2001.

E. J. Crampin, E. A. Gaffney, and P. K. Maini. Pattern formation through reaction and diffusion on growing domains: Scenarios for robust pattern formation. *Bull. Math. Biol.*, 61:1093–1120, 1999.

E. J. Crampin, E. A. Gaffney, and P. K. Maini. Mode doubling and tripling in reaction-diffusion patterns on growing domains: A piecewise linear model. *J. Math. Biol.*, 2001. in press.

G. Dewel and P. Borckmans. Effects of slow spatial gradients on dissipative structures. *Phys. Lett. A*, 138(4,5):189–192, 1989.

R. Dillon and H. G. Othmer. A mathematical model for outgrowth and spatial patterning of the vertebrate limb bud. *J. theor. Biol.*, 197:295–330, 1999.

E. Dulos, P. Davies, B. Rudovics, and P. De Kepper. From quasi-2D to 3D Turing structures in ramped systems. *Physica D*, 98:53–66, 1996.

A. Gierer and H. Meinhardt. A theory of biological pattern formation. *Kybernetik*, 12:30–39, 1972.

L. G. Harrison and M. Kolář. Coupling between reaction-diffusion prepattern and expressed morphogenesis, applied to desmids and dasyclads. *J. theor. Biol.*, 130:493–515, 1988.

L. G. Harrison, S. Wehner, and D. M. Holloway. Complex morphogenesis of surfaces: theory and experiment on coupling of reaction-diffusion patterning to growth. *Faraday Discuss.*, 120, 2001. (in press).

M. Herschkowitz-Kaufman. Bifurcation anaylsis of nonlinear reaction-diffusion equations—II. Steady state solutions and comparison with numerical simulations. *Bull. Math. Biol.*, 37:589–636, 1975.

D. M. Holloway and L. G. Harrison. Algal morphogenesis: modelling interspecific variation in *Micrasteras* with reaction-diffusion patterned catalysis of cell surface growth. *Phil. Trans. R. Soc. Lond. B*, 354:417–433, 1999.

S. Kondo and R. Asai. A reaction-diffusion wave on the skin of the marine angelfish *Pomacanthus*. *Nature*, 376:765–768, 1995.

P. M. Kulesa, G. C. Cruywagen, S. R. Lubkin, P. K. Maini, J. Sneyd, M. W. J. Ferguson, and J. D. Murray. On a model mechanism for the spatial pattering of teeth primordia in the alligator. *J. theor. Biol.*, 180:287–296, 1996.

T. C. Lacalli. Dissipative structures and morphogenetic pattern in unicellular algae. *Phil. Trans. R. Soc. Lond. B*, 294:547–588, 1981.

S. S. Liaw, C. C. Yang, R. T. Liu, and J. T. Hong. Turing model for the patterns of lady beetles. *Phys. Rev. E*, 64, 2001. (in press).

A. Madzvamuse, R. D. K. Thomas, P. K. Maini, and A. J. Wathen. A numerical approach to the study of spatial pattern formation in the ligaments of arcoid bivalves. (submitted), 2001.

P. K. Maini, D. L. Benson, and J. A. Sherratt. Pattern formation in reaction-diffusion models with spatially inhomogeneous diffusion coefficients. *IMA J. Math. Appl. Med. and Biol.*, 9:197–213, 1992.

A. May, P. A. Firby, and A. P. Bassom. Diffusion driven instability in an inhomogeneous circular domain. *Mathl. Comput. Modelling*, 29(4):53–66, 1999.

H. Meinhardt. *The Algorithmic Beauty of Sea Shells*. Springer, Heidelberg, 1995.

H. Meinhardt, A.-J. Koch, and G. Bernasconi. Models of pattern formation applied to plant development. In R. V. Jean and D. Barabé, editors, *Symmetry in Plants*, pages 723–758. World Scientific, Singapore, 1998.

J. Monod. *Recherches sur la Croissance des Cultures Bacteriennes*. Herman, Paris, 1942.

K. W. Morton and D. F. Mayers. *Numerical Solution of Partial Differential Equations*. Cambridge University Press, 1994.

J. D. Murray. *Mathematical Biology.* Springer-Verlag, Berlin, 2nd edition, 1993.

G. F. Oster and J. D. Murray. Pattern formation models and developmental constraints. *J. exp. Zool.*, 251:186–202, 1989.

K. J. Painter, P. K. Maini, and H. G. Othmer. Stripe formation in juvenile *Pomacanthus* explained by a generalised Turing mechanism with chemotaxis. *Proc. Natl. Acad. Sci. USA*, 96:5549–5554, 1999.

R. Plaza, F. Sánchez-Garduño, P. Padilla, R. A. Barrio, and P. K. Maini. The effect of growth and curvature on pattern formation. (in preparation), 2001.

J. Schnakenberg. Simple chemical reaction systems with limit cycle behaviour. *J. theor. Biol.*, 81:389–400, 1979.

H. L. Smith and P. Waltman. *The Theory of the Chemostat: Dynamics of Microbial Competition.* Cambridge University Press, 1995.

A. M. Turing. The chemical basis of morphogenesis. *Phil. Trans. R. Soc. Lond. B*, 237:37–72, 1952.

C. Varea, J. L. Aragón, and R. A. Barrio. Turing patterns on a sphere. *Phys. Rev. E*, 60(4):4588–4592, 1999.

List of Figures

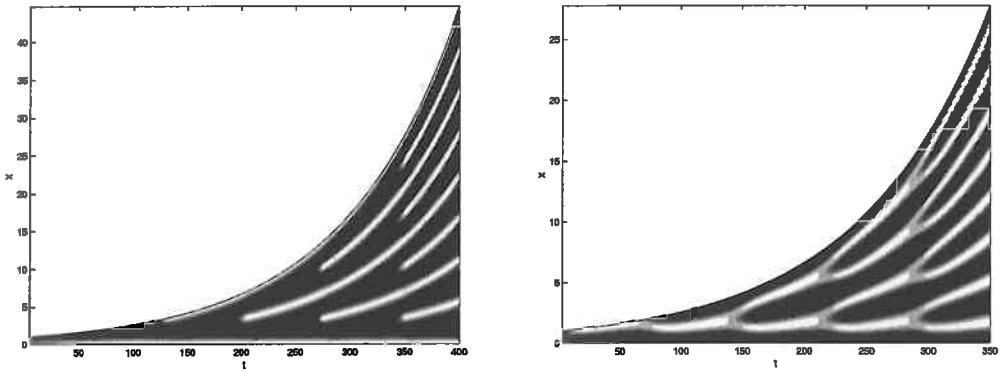

(a) (b)

Figure 1: Patterns in the activator $v(x,t)$ obtained on the uniformly growing domain. For domain expansion the patterns change regularly through frequency (or 'mode') doubling behaviour: (a) Gierer-Meinhardt kinetics, where $f(u,v) = v^2 - u$ and $g(u,v) = v^2/u - 0.5v + 0.1$, showing regular insertion of new activator peaks and (b) Schnakenberg kinetics, where $f(u,v) = 0.9 - uv^2$ and $g(u,v) = 0.1 + uv^2 - v$, showing peak splitting. In both cases $d = 0.025$, $\gamma_0 = 1.0$ and $S = \rho = 0.01$. Numerical solutions are computed using NAG library routine DO3PCF. Gray-scale is from low (black) to high (white) concentration.

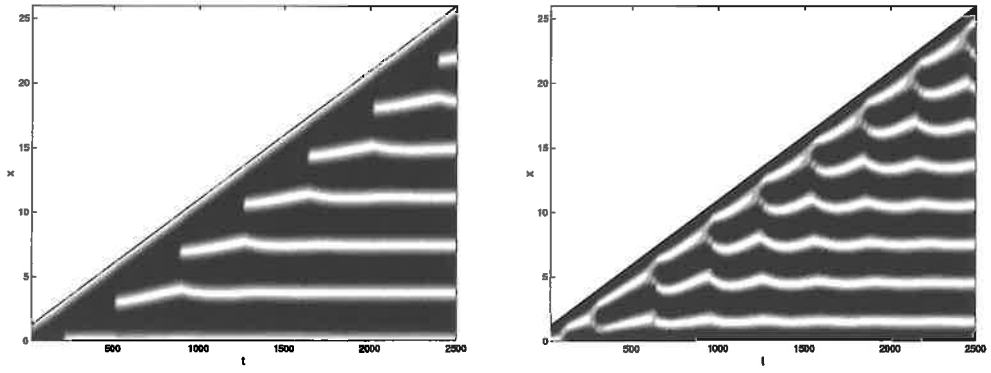

Figure 2: Patterns in the activator chemical obtained under apical growth for (a) Gierer-Meinhardt kinetics showing insertion of new activator peaks near the moving boundary and (b) Schnakenberg kinetics showing splitting of the activator peak proximal to the region of outgrowth. Kinetic functions and parameters as for figure 1 with $\delta S_{tip} = 0.01$, *i.e.* $r(t) = 1 + 0.01t$. Gray-scale is from low (black) to high (white) concentration.

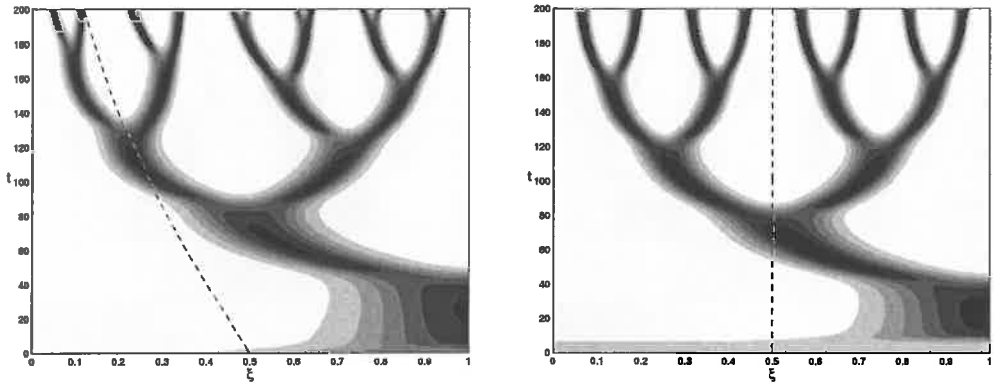

Figure 3: Asymmetric peak splitting for piecewise uniform domain growth, with Schnakenberg kinetics. Numerical solutions $v(\xi, t)$ are shown for (a) piecewise uniform domain growth with $\rho_1 = 0.01$, $\rho_2 = 0.02$ and $\gamma_0 = 1$ and (b) uniform domain growth with $\rho = 0.017$ and $\gamma_0 = 1$ giving (approximately) the same dimensional domain length at time $t = 200$. Shading is 0 (white) to 4 (black). In this and subsequent figures the initial conditions were chosen such that a right-hand boundary peak is first generated. Further numerical simulations (data not shown) demonstrate that the pattern sequence and asymmetry are the same for an initial peak located on the left-hand boundary. For ease of comparison the faster-growing sub-domain is on the right hand side.

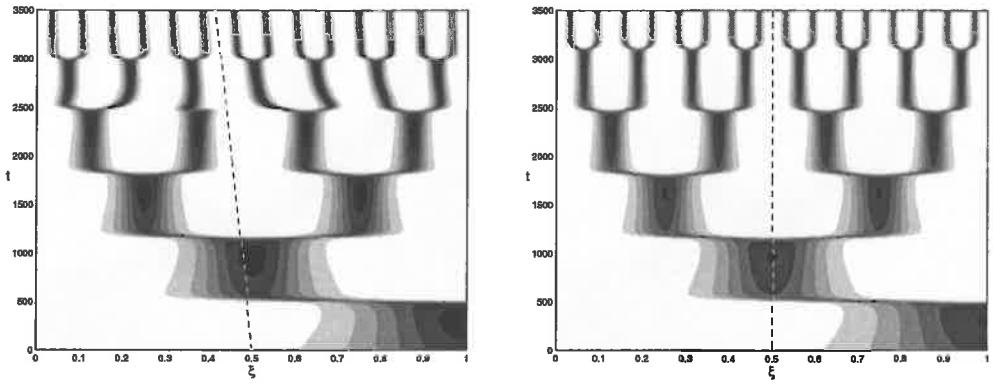

Figure 4: Missing peaks for piecewise uniform domain growth. We plot numerical solutions for the activator $v(\xi, t)$ for (a) piecewise uniform domain growth with $\rho_1 = 0.001$, $\rho_2 = 0.0011$ and $\gamma_0 = 1$ and (b) uniform domain growth with $\rho = 0.00105$ and $\gamma_0 = 1$ giving (approximately) the same dimensional domain length at time $t = 3500$. Other remarks as for figure 3.

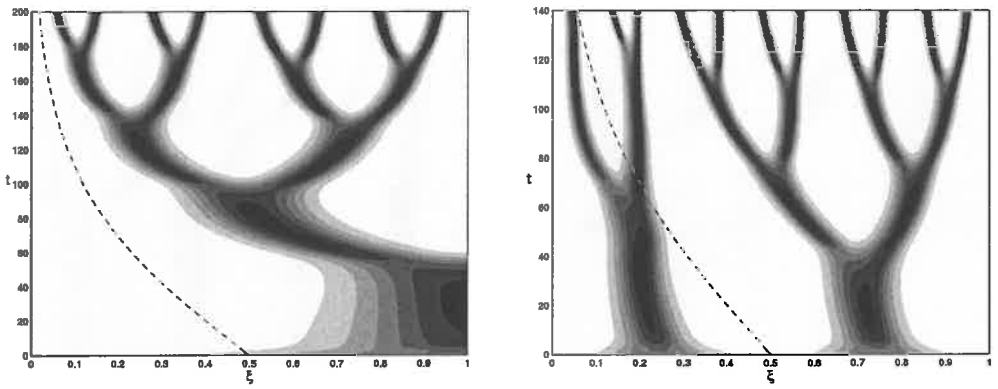

Figure 5: Pattern sequences generated from larger initial domains. We show the activator $v(\xi, t)$ for piecewise uniform domain growth with $\rho_1 = 0.0$, $\rho_2 = 0.02$ and (a) $\gamma_0 = 1.0$ so that the initial mode $m = 1$ and (b) with $\gamma_0 = 20.0$ where the initial pattern is mode $m = 4$. Other remarks as for figure 3.

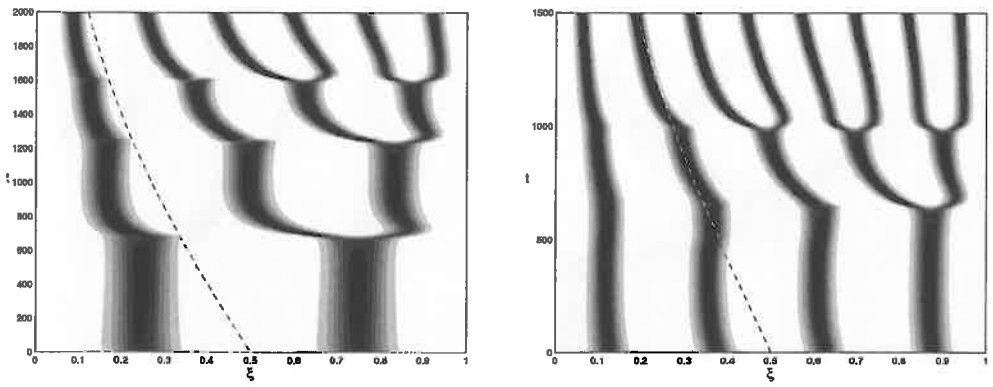

(a) (b)

Figure 6: Pattern sequences generated from larger initial domains. Numerical solutions for activator $v(\xi, t)$ are shown for piecewise uniform domain growth with $\rho_1 = 0.0$, $\rho_2 = 0.001$ and (a) $\gamma_0 = 20.0$ so that the initial mode to grow is mode $m = 4$ and (b) $\gamma_0 = 80.0$ where the initial pattern is $m = 8$. Other remarks as for figure 3.

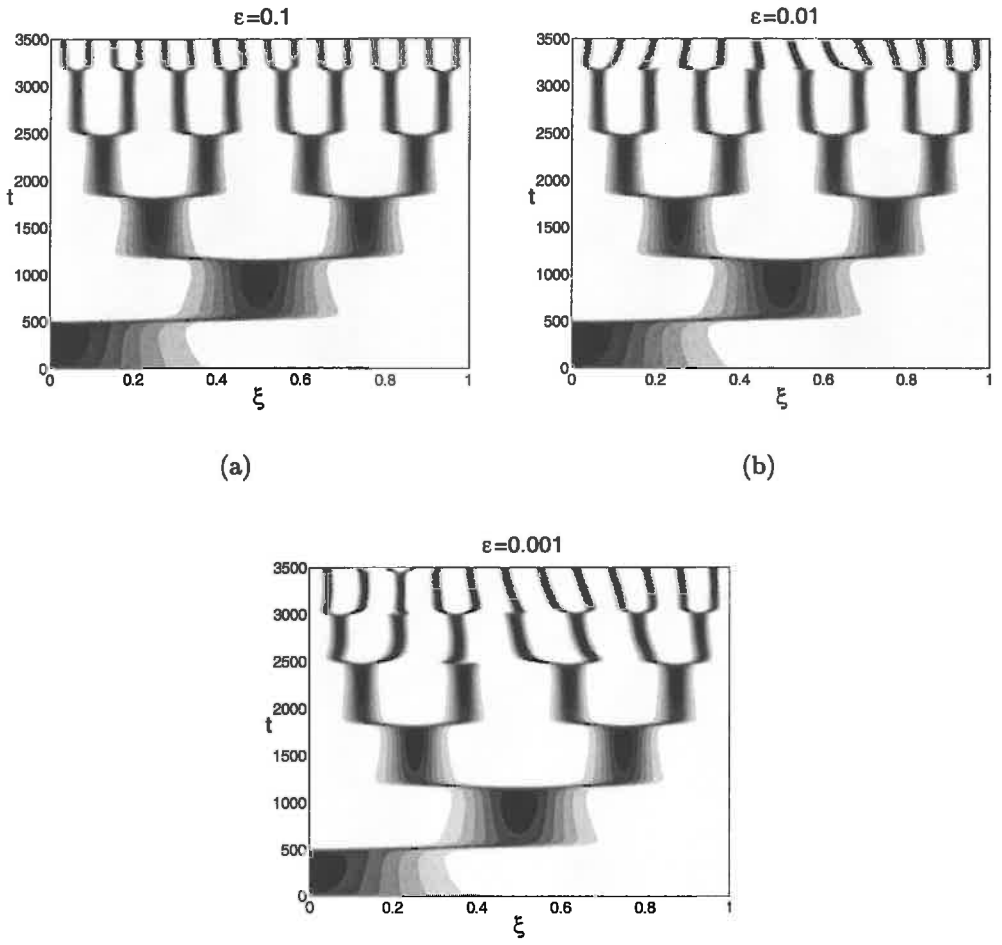

Figure 7: Pattern formation with nonuniform domain growth: as ε is reduced solutions resemble the piecewise uniform case shown in figure 4(a). Here we plot numerical solutions for the activator $v(\xi, t)$ with the *tanh* function for the domain growth and $\rho_1 = 0.001$, $\rho_2 = 0.0011$ and $\Theta = 0.5$. The initial domain length $\gamma_0 = 1$ and we plot solutions for (a) $\varepsilon = 0.1$, (b) $\varepsilon = 0.01$ and (c) $\varepsilon = 0.001$ giving successively better approximations to the piecewise uniform case.

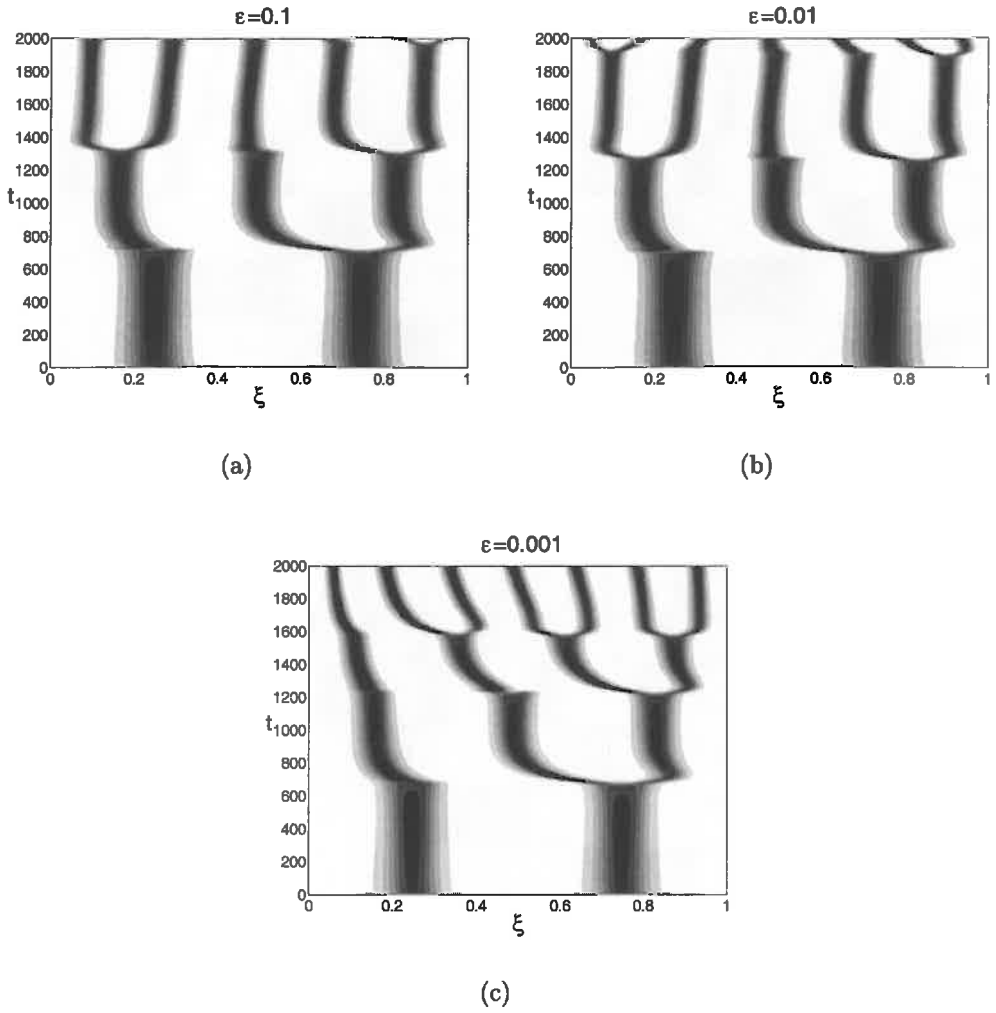

Figure 8: Pattern formation under nonuniform domain growth for larger initial domains. Numerical solutions are shown for the activator $v(\xi, t)$ with the *tanh* function for the domain growth and $\rho_1 = 0$, $\rho_2 = 0.001$ and $\Theta = 0.5$. The initial domain length is $\gamma_0 = 20$ and we plot (a) $\varepsilon = 0.1$, (b) $\varepsilon = 0.01$ and (c) $\varepsilon = 0.001$.

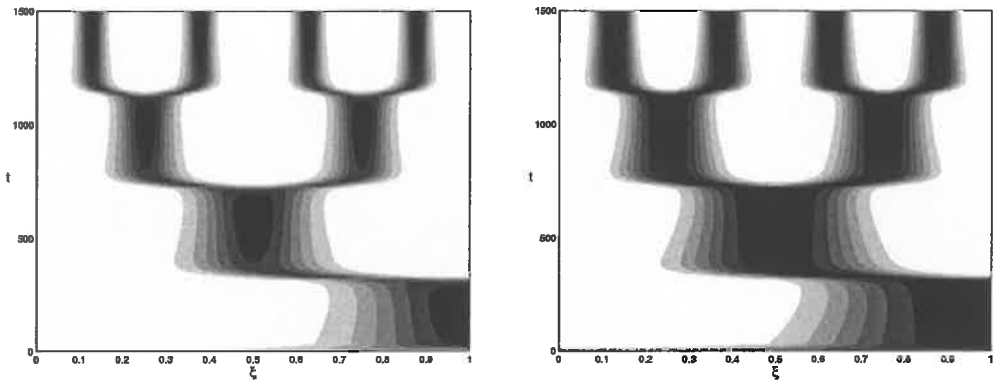

Figure 9: Pattern formation with reactant-controlled domain growth. We plot (a) the activator (the 'growth factor') solution on the scaled domain and (b) the local strain rate (rate of volumetric change), for Schnakenberg kinetics and with $\gamma_0 = 1$, $d = 0.01$, $\rho = 0.005$, $\kappa = 1$ and $m = 1$. We have taken $\alpha = 0$ although we have found no qualitative change to the results for small non-zero α. The numerical mesh has 1000 space points and no change to the solution is found by halving the mesh size. Numerical solutions were also computed with sigmoidal response functions for higher cooperativity, $m > 1$, and for other values of κ, giving qualitatively similar results.

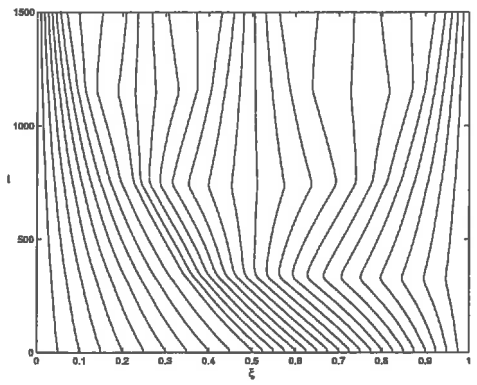

Figure 10: Flow lines, $\Gamma(X,t)/\Gamma(1,t)$, for reactant-controlled domain growth. The lines represent the trajectories of particles initially separated at regular intervals in X. For clarity twice as many points are taken in the second half as in the first half of the interval $X \in [0,1]$. Parameters and other details as in figure 9.